Hindawi
Complexity
Volume 2018, Article ID 2517987, 13 pages
https://doi.org/10.1155/2018/2517987

Research Article

Adaptive Robust Method for Dynamic Economic Emission Dispatch Incorporating Renewable Energy and Energy Storage

Tingli Cheng,[1] **Minyou Chen**,[1] **Yingxiang Wang**,[1] **Bo Li**,[1] **Muhammad Arshad Shehzad Hassan**,[1] **Tao Chen**,[2] **and Ruilin Xu**[2]

[1]*State Key Laboratory of Power Transmission Equipment & System Security and New Technology, School of Electrical Engineering, Chongqing University, Chongqing 400044, China*
[2]*State Grid Chongqing Electric Power Research Institute, Chongqing 400021, China*

Correspondence should be addressed to Tingli Cheng; tingli_cheng@126.com

Received 16 March 2018; Accepted 10 April 2018; Published 26 June 2018

Academic Editor: Liang Hu

In association with the development of intermittent renewable energy generation (REG), dynamic multiobjective dispatch faces more challenges for power system operation due to significant REG uncertainty. To tackle the problems, a day-ahead, optimal dispatch problem incorporating energy storage (ES) is formulated and solved based on a robust multiobjective optimization method. In the proposed model, dynamic multistage ES and generator dispatch patterns are optimized to reduce the cost and emissions. Specifically, strong constraints of the charging/discharging behaviors of the ES in the space-time domain are considered to prolong its lifetime. Additionally, an adaptive robust model based on minimax multiobjective optimization is formulated to find optimal dispatch solutions adapted to uncertain REG changes. Moreover, an effective optimization algorithm, namely, the hybrid multiobjective Particle Swarm Optimization and Teaching Learning Based Optimization (PSO-TLBO), is employed to seek an optimal Pareto front of the proposed dispatch model. This approach has been tested on power system integrated with wind power and ES. Numerical results reveal that the robust multiobjective dispatch model successfully meets the demands of obtaining solutions when wind power uncertainty is considered. Meanwhile, the comparison results demonstrate the competitive performance of the PSO-TLBO method in solving the proposed dispatch problems.

1. Introduction

The traditional economic dispatch method aims to determine a generation schedule that minimizes total generation cost while being subjected to generator and system operating limits [1–3]. With increasing concerns of environmental pollution, harmful emissions, such as SO_2, NO_x, CO, and CO_2, have attracted widespread attention. Therefore, simultaneously minimizing total generation cost and emissions has become a crucial research topic. In some studies, the separate economic and environmental dispatch problems are converted to an economic and emission dispatch (EED) problem, formulating a multiobjective optimization issue [3–5]. The EED can provide a set of dispatch solutions for decision marker to choose from with different preferences in economic and emission. Many methods and approaches have been proposed to solve the multiobjective EED problem [6–13]. In the initial studies [6–8], researchers attempted to transform the EED problem into a single-objective model based on a linear combination of different objectives as a weighted sum. However, this method cannot obtain Pareto front solutions in a single run and does not address how to select weighting factors for the system operators. Moreover, these approaches fail to achieve optimal solutions when the objective functions are not convex or when the objective functions have a discontinuous variable space. To address these problems, several artificial intelligent techniques have shown good performance. An improved Hopfield neural network (NN) in [9] and an improved back-propagation NN in [10] were reported to optimize EED problems. However, these approaches are readily trapped within the local optimum, since the achieved results are not sufficiently accurate. On the other hand, multiobjective evolutionary algorithms have been successfully applied to solve the EED problem

[3, 11, 12]. In [3], a novel modified adaptive θ-particle swarm optimization is presented to investigate the multiobjective EED. The fuzzy IF/THEN rule is used to self-adaptively adjust the cognitive and social parameters in the PSO to avoid the evolution stagnation for continuous generation. Reference [11] presents a multiobjective differential evolution algorithm for EED problems. In [12], a robust EED model based on an effective function is built to handle wind power uncertainties. Carbon capture and storage are considered in the model formulation to reduce carbon emission, and a multiobjective bacterial colony chemotaxis method is adopted to solve the proposed robust EED model. However, none of these papers consider energy storage (ES) integration.

Due to the long-term fossil fuel energy crisis and the recent Paris agreement tasks to reduce fossil fuel dependency in traditional power generation, significant renewable energy generation (REG), for example, wind power, photovoltaic energy, and tidal energy, is integrated into multiple levels of the power grid. The uncertainty and variability of the power production provided by REG raise the risk of system instability, particularly in distribution networks. To solve this problem, the integration of ES is an effective solution to alleviate the negative effects caused by the intermittent nature of REG. According to reviews [14–16], ES plays a vital role in smoothing the production of REG, improving the REG penetration level and peak shaving, ensuring system reliability, and increasing the economic and environmental benefits of the power system [17]. Improper dispatch scheduling of generation may lead to undesired cost increases or system reliability deterioration. Typical ES has dynamic power and energy formulations in which the constraints are coupled along the time and space domain. The operation of ES in one time step affects the evolving operation in the other time slots. Therefore, a multistage EED integrated with ES is a strong coupling and dynamic problem in the space-time domain [18, 19].

In past studies, some economic or EED dispatch approaches are presented. First, some literature has focused on economic ES dispatch or EED focused on single-interval (1 hour) dispatch [12, 20, 21]. In this setup, the economic or emission objectives in one time interval are optimized and then shifted to the next time interval. Second, in day-ahead scheduling problems, current research is focused on investigating the composite economic cost with ES within multiperiods [22–25]. Multiobjective, multistage, dispatch optimization problems with ES are rarely considered. In addition, the prediction error in day-ahead REG prediction is inevitable in real cases, which should be carefully taken into consideration in the EED process. At the most time, chance constraint is used to ensure that the loss of load probability is lower than predefined risk level to deal with uncertain REG problems [26, 27]. However, it is difficult to obtain the distribution function of REG.

To the best of the authors' knowledge, very few researchers emphasized the study on ES scheduling in dynamic, multiperiod, EED while simultaneously dealing with the uncertainty of intermittent REG [17]. Motivated by the above concerns, this paper proposes a dynamic EED approach to schedule the output of ES together with controllable generations over the next 24-hour time span. The main contributions of this paper are organized as follows. (i) To address the uncertainties of REG, robust multiobjective optimization is proposed based on minimax optimization approach. (ii) The EED dispatch problem with REG prediction error is converted to a robust multiobjective dispatch model. (iii) Aiming at effectively solving the proposed model, a novel multiobjective PSO-TLBO is proposed and employed to seek the Pareto solutions.

The organization of this paper is decomposed into seven sections. Section 2 introduces the energy storage model followed by the day-ahead generators and ES dispatch problem formulation presented in Section 3. Further, the robust, multiobjective, day-ahead dispatch model is explained in Section 4. Section 5 proposes the multiobjective algorithm to solve the given complex problem. The numerical case study and conclusions are then presented in Sections 6 and 7, respectively.

2. Energy Storage Model

ES is connected to the gird by converters capable of flexibly operating in charge and discharge modes [25, 28]. It is therefore promising for ES to handle the intermittent REG integration problem and to improve the flexibility of energy dispatch. However, ES has significant dynamic and evolving power and energy characteristics, leading to a batch of technical limits with time-evolving decision variables, particularly in multistage scheduling operation [22]. Details of the ES general model and its dynamic constraints are expressed as follows [29].

ES charge/discharge power limits are as follows:

$$\begin{aligned} -P_{\mathrm{ES},i} \le P_{\mathrm{ch},i}(t) \le 0, \\ 0 \le P_{\mathrm{dis},i}(t) \le P_{\mathrm{ES},i}, \end{aligned} \tag{1}$$

where $P_{\mathrm{ch},i}(t)$ and $P_{\mathrm{dis},i}(t)$ denote the charge and discharge power of the ith ES at the hour t, with the power output of ES being positive when discharging, and vice versa. $P_{\mathrm{ES},i}$ is the power capacity of ith ES.

The state of charge (SOC) is a crucial state variable in the process of ES schedule and operation.

When the ES is charging ($P(t) < 0$),

$$S_{\mathrm{oc},i}(t+1) = S_{\mathrm{oc},i}(t) - \frac{\eta_c P(t)\,\Delta t}{E^{\max}}. \tag{2}$$

When the ES is discharging ($P(t) > 0$),

$$S_{\mathrm{oc},i}(t+1) = S_{\mathrm{oc},i}(t) - \frac{P(t)\,\Delta t/\eta_D}{E^{\max}}. \tag{3}$$

When the ES is idling ($P(t) = 0$),

$$S_{\mathrm{oc},i}(t+1) = S_{\mathrm{oc},i}(t), \tag{4}$$

where $S_{\mathrm{oc},i}(t)$ is the SOC of the ith ES at the hour t, $P(t)$ is the charge or discharge power at the hour t, η_c is the charging efficiency, η_D is the discharging efficiency, Δt is the schedule interval, and $E^{\max}$ is the ES energy capacity.

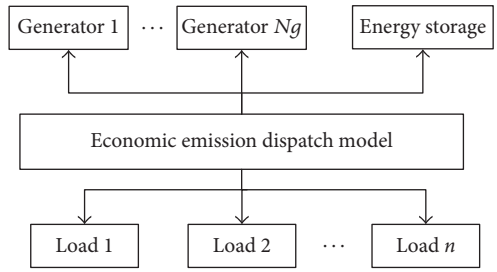

FIGURE 1: Scheme of economic emission dispatch problem.

The ES SOC limits are as follows:

$$S_{\mathrm{oc,min}} \le S_{\mathrm{oc},i}(t) \le S_{\mathrm{oc,max}}, \tag{5}$$

where $S_{\mathrm{oc},i}(t)$ is the SOC of the ith ES at the hour t, and $S_{\mathrm{oc,min}}$ and $S_{\mathrm{oc,max}}$ are the minimum and maximum limits of the SOC, respectively.

The initial SOC of each ES is the same at the beginning of each day, where T stands for all the time slots [30].

$$S_{\mathrm{oc},i}(T) = S_{\mathrm{oc},i}(0). \tag{6}$$

To prolong the lifetime of the ES, it is assumed that it is only eligible for one charge-discharge cycle per day for optimal operation [31, 32]. Meanwhile, in this paper, ES is used for peak shaving. It stores energy during off-peak and return the power during peak-load hours.

3. Problem Formulation

The day-ahead dispatch performs the generation dispatch every 24 hours, scheduling all generators and ES units the next day in hourly time slots [33, 34]. The scheme of EED model is illustrated in Figure 1. This is a typical, dynamic, multiperiod decision problem. The decision variables at each hour influence the decisions at the remaining hours. The dynamic multiobjective dispatch problem is described as follows.

3.1. Variables. The input variables of the dispatch problem are the REG power, load demand, and ES parameters over the planning period. The decision (control) variables set P is the power outputs of all the controllable units.

$$P = \left[P_1(1) \cdots P_1(T) \cdots P_i(t) \cdots P_N(t) \cdots P_N(T)\right], \tag{7}$$

where $P_i(t)$ stands for the power generation of the ith unit at the time slot t, N is the number of control variables, and T presents the total number of time slots.

3.2. Objective Function. The overall objective function of the day-ahead dispatch problem includes the total generation cost of the whole system f_1 and the pollutant emissions f_2.

$$\min f = (f_1, f_2). \tag{8}$$

The controllable generations are the fuel-based generators. The operational costs of renewable generation and ES within the short-term dispatch optimization horizon under strong constraints mentioned above are ignored [22]. Therefore, the first objective f_1 is the accumulated economic cost of all the conventional generators. These generation costs are normally modeled using a quadratic function of their power outputs [27]. The economic objective is minimized over the scheduling period, for example, 24 hours of the next day, which can be described as follows:

$$f_1 = \sum_{t=1}^{T}\left(\sum_{i=1}^{N_G}\left(a_i {P^2}_i(t) + b_i P_i(t) + c_i\right)\right). \tag{9}$$

The environmental objective is to minimize the total emission pollutants of all generators as much as possible. These emission costs are also formulated as a quadratic function of their power outputs [27], and the emissions of the ES are taken to be zero. The objective function f_2 is expressed as follows:

$$f_2 = \sum_{t=1}^{T}\left(\sum_{i=1}^{N_G}\left(\alpha_i {P^2}_i(t) + \beta_i P_i(t) + \gamma_i\right)\right). \tag{10}$$

In (9) and (10), T is the total number of time slots for next day, which is 24 hours in this paper, N_G is the number of conventional generators, a_i, b_i, c_i are the cost coefficients of the generators, and α_i, β_i, γ_i are the emission coefficients of the generators.

3.3. Technical Constraints. To maintain the power grid operation, a set of equation and in-equation constraints should be considered. The system constraints include the overall system constraints and the ES constraints. The ES constraints are shown in Section 2, and the overall system constraints are expressed as follows.

(1) Power flow balance constraint is

$$\sum_{i=1}^{N_G} P_i(t) = \sum_{i=1}^{l} L_i(t) + P_{\mathrm{loss}}(t) - P_{\mathrm{REG}}(t) - \sum_{i=1}^{N_{\mathrm{ES}}} P_i^{\mathrm{ES}}(t), \tag{11}$$

$$P_{\mathrm{loss}}(t) = \sum_{i=1}^{N_G}\sum_{j=1}^{N_G} P_i(t) B_{ij} P_j(t), \tag{12}$$

where $P_{\mathrm{REG}}(t)$, $P_i(t)$, and $P_i^{\mathrm{ES}}(t)$ are the active power injected by the REG, ith controllable generator, and ith ES at time t, respectively; N_G, N_{ES}, and l are the total number of controllable generator, energy storage, and load, respectively; B is the power loss coefficient.

(2) Generation output limits are

$$P_{i,\mathrm{min}} \le P_i(t) \le P_{i,\mathrm{max}} \quad (i = 1, 2, \ldots, N_G). \tag{13}$$

(3) Generators ramp up and down limits are

$$\begin{aligned} &P_i(t) - P_i(t-1) \le \mathrm{UR}_i, \\ &P_i(t-1) - P_i(t) \le \mathrm{DR}_i, \\ &\qquad (i = 1, 2, \ldots, N_G), \end{aligned} \tag{14}$$

where $P_{i,\min}$ and $P_{i,\max}$ represent the minimum and maximum power output of ith generator, respectively; UR_i and DR_i are the ramp up and ramp down limits for ith generator, respectively.

4. Robust Multiobjective Day-Ahead Dispatch

It is well known that renewable energy is intermittent and uncertain. The error in REG prediction is inevitable for any prediction technique. Hence, dealing with the uncertainty of renewable energy is a key issue.

4.1. Worst-Case Based Optimization. The robust optimization with the worst-case scenario is one of the most common approaches. The worst-case optimization, in a minimization problem, can be formulated as follows:

$$\min_{x\in X} \max_{p\in P} f(x, p), \tag{15}$$

where x is the decision variable over a feasible region X and p is an uncertain parameter in the uncertainty set P.

For environmental uncertainties, the function values of $f(x)$ become $F(x)$ [35, 36]:

$$F(x) = f(x, y, p), \quad p = c + \delta, \tag{16}$$

where $x = [x_1, \ldots, x_n]$ are the decision variables and $y = [y_1, \ldots, y_m]$ are the configuration variables, defined by $y = \varphi(x)$. c is the nominal value of the environmental parameter and δ is the change condition. Once a decision variable x is implemented, the configuration variable y can be termed as the solution's adaptability. The value of y will be determined according to uncertain environmental parameter. The above robust optimization with the worst-case method is focused on the best decision to worst-case performance and to minimize the risk of severe consequences.

4.2. Robust Multiobjective Optimization. Most robust optimal dispatch problems considering REG uncertainty are single-objective models or are converted from the multiobjective EED problems to a single objective. They ignore the importance of Pareto optimality, which could provide multiple optimal solutions for operators in the dispatch decision-making process. Robust optimization means to search for the solution that is the least sensitive to perturbations of the decision variables in its neighborhood [12]. The REG forecast error is unavoidable, resulting in the possibility that the optimal deterministic solutions may not be practically suitable in reality. On the other hand, stochastic methods based on the probability model have difficulty obtaining accurate probability functions. In this paper, we utilize the minimax multiobjective optimization method based on the worse case in day-ahead generator and ES dispatch problems.

We assume a robust, multiobjective optimization problem:

$$\begin{aligned} &\min F(X) = \left(f_1\left(X, Y, P'\right), \ldots, f_k\left(X, Y, P'\right)\right), \\ &P_i' = P + \delta_i;\ X \in \Omega,\ Y \in \Omega_y, \end{aligned} \tag{17}$$

where X, Y, and P' are the decision, configuration, and uncertain input variables, respectively, f_k is the kth objective function, $\delta = (\delta_1, \delta_2, \ldots, \delta_n)$ denotes the perturbation points, and Ω and Ω_y are the feasible space of X and Y.

The following robust multiobjective optimization approach is defined in (18), where a robust multiobjective solution, X^*, is defined as the Pareto-optimal solution with respect to a δ-neighborhood:

$$\min F(X) = \left(f_1^{\mathrm{Ro}}(X), f_2^{\mathrm{Ro}}(X), \ldots, f_k^{\mathrm{Ro}}(X)\right). \tag{18}$$

Subject to $X \in \Omega$, where Ω is the feasible region of the decision variables, the function $f_k^{\mathrm{Ro}}(X)$ is defined as follows:

$$\begin{aligned} f_k^{\mathrm{Ro}}(X) = \max &\left(f_k(X, Y, P + \delta_1) \cdots f_k(X, Y, P + \delta_i)\right. \\ &\left. \cdots f_k(X, Y, P + \delta_n)\right), \end{aligned} \tag{19}$$

where n denotes the sampling point number in the perturbation domain and δ_i is the ith perturbation sampling point.

4.3. Robust EED Dispatch. In the day-ahead predispatch stage, the intermittent renewable power, such as wind, usually deviates from its forecasted value. The forecast error of an REG exists in any prediction models. In view of this, a robust EED dispatch model is developed to adapt to the uncertainty of wind power (WP) and handle its prediction error when spinning reserve is not considered. In order to balance the generated power with the power demand and power loss, one of generators is chosen as the slack generator with output limits. According to (11) and (12), the power output of the slack generator, $P_1(t)$, can be calculated by solving the following quadratic equation [37]:

$$\begin{aligned} 0 &= B_{11} P_1^2(t) + \left(2\sum_{i=2}^{Ng} B_{1i} P_i(t) - 1\right) P_1(t) \\ &\quad + \left(P_D(t) + \sum_{i=2}^{Ng}\sum_{i=2}^{Ng} P_i(t) B_{ij} P_j(t) - \sum_{i=2}^{Ng} P_i(t)\right), \\ P_D(t) &= \sum_{i=1}^{l} L_i(t) - P_{\mathrm{REG}}(t) - \sum_{i=1}^{N_{\mathrm{ES}}} P_i^{\mathrm{ES}}(t). \end{aligned} \tag{20}$$

According to (20), once the other controlled units is determined, the output of the slack generator $P_1(t)$ is temporarily fixed. $P_1(t)$ is regarded as a configuration variable. Then, the adaptive adjustment of the slack generator output, associated with other fixed control variables, allows the robust dispatch solutions to follow other operational conditions. In other words, only the output of the slack generator $P_1(t)$ will be adjusted with robust optimal dispatch solutions according to the realization of different REG output.

Sampling H schemes ($P_{WP}(t)$) for each time slot ($t = 1, 2, \ldots, 24$) for WP generation with certain error by LHS;
$P_{WP,min}(t) = \max(\min(P_{WP}(t)), 0, \overline{P}_{WP}(t) - 1.96\delta(t))$;
$P_{WP,max}(t) = \min(\max(P_{WP}(t)), \overline{P}_{WP}(t) + 1.96\delta(t), P_{WP,cap})$;
$P_{WP}(t) = \max(\min(P_{WP}(t), P_{WP,max}(t)), P_{WP,min}(t))$;
The first extreme scenario:
$\mathrm{WP}_{(1)} = \bigcup_{t \in T} P_{WP,min}(t) \quad (T = \{1, 2, \ldots, 24\})$;
The second extreme scenario:
$\mathrm{WP}_{(2)} = \bigcup_{t \in T} P_{WP,max}(t) \quad (T = \{1, 2, \ldots, 24\})$;
Other $n - 2$ stochastic scenarios:
For $i = 3 : n$
Randomly select $P_{WP,stochastic}(t)$ from samples of $P_{WP}(t)$;
$\mathrm{WP}_{(i)} = \bigcup_{t \in T} P_{WP,stochastic}(t) \quad (T = \{1, 2, \ldots, 24\})$;
End for

Algorithm 1: 24-hour WP scenarios selection.

The original EED dispatch objective functions that minimize cost and emissions in (9) and (10) are transformed in the robust model, which can be expressed as follows:

$$\begin{aligned} f_1^{\mathrm{RO}}(P) &= \max\left(f_1(P, P_{WP} + \delta_1), f_1(P, P_{WP} + \delta_2)\right. \\ &\left.\cdots f_1(P, P_{WP} + \delta_n)\right) = \max\left(f_1(P, P_{WP}(\delta))\right), \\ &\qquad \delta \in \{\delta_1, \delta_2 \cdots \delta_n\}, \\ f_2^{\mathrm{RO}}(P) &= \max\left(f_2(P, P_{WP} + \delta_1), f_2(P, P_{WP} + \delta_2)\right. \\ &\left.\cdots f_2(P, P_{WP} + \delta_n)\right) = \max\left(f_2(P, P_{WP}(\delta))\right), \\ &\qquad \delta \in \{\delta_1, \delta_2 \cdots \delta_n\}, \end{aligned} \tag{21}$$

where P is the power output of controllable power units and $P_{WP}(\delta)$ is the uncertain set of WP.

The robust day-ahead EED dispatch model is expressed as follows:

$$\min\left(f_1^{\mathrm{RO}}, f_2^{\mathrm{RO}}\right). \tag{22}$$

The constraints are formulated as (1)–(6) and (11)–(14).

4.4. Uncertainty Wind Power. To further analyze the uncertainty of WP, the actual WP output at time t ($P_{WP}(t)$) limits can be described as follows:

$$0 \le P_{WP}(t) \le P_{WP,cap}. \tag{23}$$

Commonly, the minimum output of WP is 0, and the maximum is defined as the installed capacity.

In the robust optimization, the uncertainty has a direct impact on its performance. WP generations follow the Gaussian distribution, with the predicted value as the mean $\overline{P}_{WP}(t)$ and prediction error $\delta(t)$ as the standard variance. A 95% percentage of $P_{WP}(t)$ samples fall in the range $[\overline{P}_{WP}(t) - 1.96\delta(t), \overline{P}_{WP}(t) + 1.96\delta(t)]$. To generate typical scenarios, Latin hypercube sampling (LHS) has been utilized to generate WP uncertain dates each time slot [38]. To efficiently capture f_1^{RO} and f_2^{RO} with uncertainty in 24-hour time slots in (21), two extreme scenarios, as well as several stochastic scenarios, are selected using LHS. To ensure robust optimal solutions, the method to obtain 24-hour WP scenarios is shown as Algorithm 1.

5. Multiobjective PSO-TLBO to Solve the Problem

The robust dispatch problem is formulated as a mathematic model, and the task in this section is to rapidly and effectively seek a balance between the total economic and emission benefits over all intervals during the next day. We adopt a novel, multiobjective, metaheuristic based method called the PSO-TLBO to solve the problem.

5.1. Multiobjective PSO-TLBO. To find the optimal solutions in the aforementioned multistage, day-ahead dispatch problem, an effective and efficient multiobjective optimization method is required. It is noted that PSO is a popular technique but lacks sufficient exchange within different particles. Its premature convergence limits the performance of the MOPSO [39]. The multiobjective Teaching Learning Based Optimization (TLBO) can achieve the satisfactory performance on some benchmark functions with respect to convergence rate and calculation time but sometimes weak in diversity and distribution, especially in nonconvex Pareto functions and multimodal function [40]. Meanwhile, EED dispatch problem has lots of equation and in-equation constraints. When energy storages with strong coupling constraints incorporated into EED, EED problem becomes more complex. The current multiobjective PSO or TLBO cannot simultaneously capture satisfactory optimal solutions with respect to good convergence and well-spread goals for such a complex EED problem. To capture better dynamic and robust EED schemes, the effective PSO update is employed for the global search and gives a good direction to the optimal region. In addition, the TLBO algorithm is activated periodically to improve the exploration and exploitation ability

of the PSO. Meanwhile, a circular crowded sorting (CCS) strategy is proposed to truncate the nondominated solutions archive. The multiobjective PSO-TLBO is implemented in [41].

5.2. Constraints Handling. To satisfy the power balance in (11), one generator is assumed to be in slack generator operation, and the limit constraints will be handled using the static penalty method [37]. The constraints of other generators and ES outputs will be handed using their boundaries. If the dimension of the particle moves outside of its boundaries, it will be assigned the value of the corresponding boundary. The constraint of the ES charge/discharge power will be handled by the following equations:

$$P_{\mathrm{ch},i}(t) = \max\left(P_{\mathrm{ch},i}(t), -P_{\mathrm{ES},i}, \left(S_{\mathrm{oc,min}} - S_{\mathrm{oc},i}(t)\right) \times \frac{E^{\max}}{\eta_c}\right), \quad (24)$$

$$P_{\mathrm{dis},i}(t) = \min\left(P_{\mathrm{dis},i}(t), P_{\mathrm{ES},i}, \left(S_{\mathrm{oc,max}} - S_{\mathrm{oc},i}(t)\right) \times E^{\max} \times \eta_D\right).$$

The slack generator limits, generator ramp limits and SOC level in the end constraint will be handled using the static penalty method with the penalty function below. The penalty function will be expressed as (25) when the constraints are violated:

$$f_v = C\sum_{i=1}^{N}\delta_i, \quad (25)$$

where N is the total number of constraints handled using the static penalty method, and C is the penalty coefficient ($C = 1E5$ in subsequent simulation of this paper). $\delta = 0$ if there are no constraint violations in the given variable and $\delta = 1$ if a constraint is violated for a given variable. The penalty function will be added to the objective function, and the infeasible particles have a lower chance to be selected.

5.3. Solution Framework of the Dispatch Problem. The outline of the multiobjective PSO-TLBO to solve the robust day-ahead EED problem is presented as follows.

Step 1. Choose the appropriate parameters of the multiobjective PSO-TLBO, such as the population size, the maximum iteration numbers, inertia weight, and social coefficient.

Step 2. Initialize all particles in the swarm randomly and ensure that the positions of the particles are in the problem space.

Step 3. Obtain the REG prediction data during the 24 hours of the next day. Obtain the robust day-ahead EED model from Section 4. Update the particle positions according to the multiobjective PSO-TLBO from Section 5.1. Compute the fitness (f_1^{Ro}, f_2^{Ro}) (objective functions) of all particles in the swarm.

Table 1: Algorithm parameters.

Size	Population 100, archive 50
Iterations	Maximum 200
Other Parameters	TV-MOPSO [42], PSO-TLBO [41] ($D1 = 1, D2 = 1, \mathrm{INV} = 7$): $w_1 = 0.7, w_2 = 0.4, c_{1i} = 2.5, c_{1f} = 0.5, c_{2i} = 0.5, c_{2f} = 2.5$

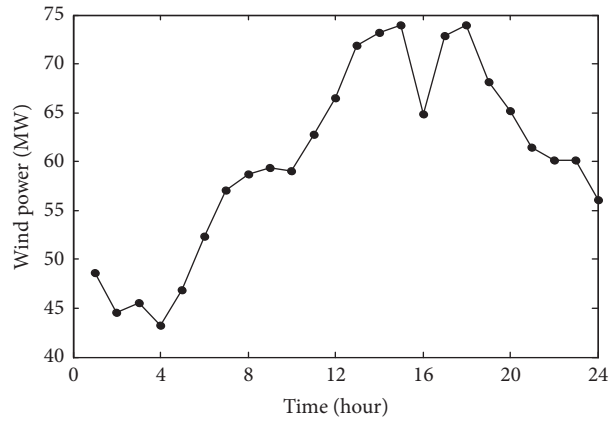

Figure 2: Predicted wind power for the 24 hours, next day.

Step 4. Judge the constraints of the control and state variables. If constraints are violated, handle the constraints with the references from Section 5.2.

Step 5. Iterative process continues if the maximum iteration is not reached. Otherwise, output the optimal Pareto solutions.

6. Case Study

The six generators bus system is used for the case study. The algorithm parameters are listed in Table 1. The detailed generator limit and the economic and emission coefficients [27] are shown in Table 2. Generator G1 is assumed to be a slack generator. A wind farm is connected and its prediction power production for the 24 hours next day is shown in Figure 2. The prediction load information in the next 24 hours is illustrated in Figure 3. It is assumed that load prediction is accurate. The storage is incorporated with a capacity of 200 MWh and maximum charge/discharge power is 80 MW. The charge and discharge efficiencies of ESS are 92%. It is assumed that the initial SOC is 0.5 before day-ahead dispatch, and the limit of the SOC is [0.2, 1].

To verify the efficiency of the robust EED optimization in the dispatch problem with ES, three cases are tested.

Case 1. The deterministic EED with ES test without WP prediction error is considered.

Case 2. The robust EED with ES test with different WP prediction errors is considered.

Case 3. Repeat Cases 1 and 2 without ES, respectively.

Table 2: Generator parameters.

Generators	G1	G2	G3	G4	G5	G6
P_{min} (MW)	10	15	15	15	15	15
P_{max} (MW)	200	170	150	180	130	120
UR (MW/h)	60	40	40	40	40	40
DR (MW/h)	60	40	40	40	40	40
Cost						
a (\$/(MW)^2 h)	0.00375	0.0175	0.0625	0.00834	0.025	0.025
b (\$/MWh)	2	1.75	1	3.25	3	3
c (\$/h)	0	0	0	0	0	0
Emission						
α (lb/(MW)^2 h)	0.0649	0.05638	0.04586	0.03380	0.04586	0.05151
β (lb/MWh)	−0.05554	−0.06047	−0.05094	−0.03550	−0.05094	−0.05555
γ (lb/h)	0.04091	0.02543	0.04258	0.05326	0.04258	0.06131

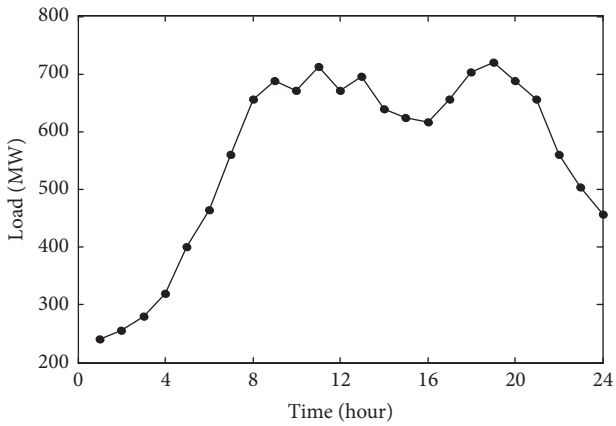

Figure 3: Predicted load demand for the 24 hours, next day.

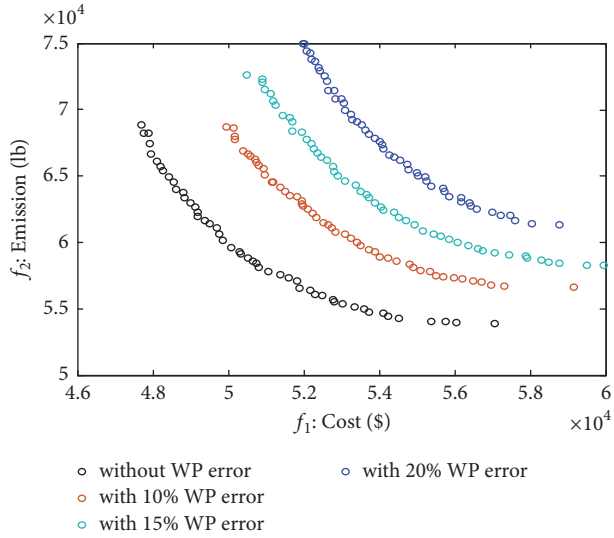

Figure 4: Pareto fronts obtained from the PSO-TLBO in Cases 1 and 2.

6.1. Simulation Results of Cases 1 and 2. For comparison, the Pareto fronts obtained from the deterministic EED without WP prediction error in Case 1 and with WP prediction errors of 10%, 15%, and 20% in Case 2, both of which use the PSO-TLBO, are shown in Figure 4. We can see from Figure 4 that there is a shift in the Pareto front in Case 2 from the Pareto front in Case 1 without the WP prediction error. This means that the acquisition of the robustness is at the expense of a greater generation cost and more emissions. It is clear that as the WP prediction error increases, the gap between the robust Pareto fronts in Case 2 and original front in Case 1 enlarges. This reveals that more accurate WP prediction techniques result in lower costs and emissions.

The aforementioned results can be understood as follows. In Case 1, the output of the generator and ES is controlled to satisfy the power consumption and to maintain the system reliability while ensuring that all equations and inequation constraints are satisfied. In the robust EED with WP prediction in Case 2, the methods attempt to find the best Pareto fronts under the worst-case problem, for example, to minimize the maximum objective values in (21). In this situation, the generators and ES dispatch have to remarkably change their output when the WP shows dramatic changes. Compared with the deterministic EED in Case 1, the robust EED has to schedule with more costs and emissions when dealing with the uncertainty of the WP.

6.2. Robustness Analysis. To obtain the extreme and stochastic scenarios in uncertainty sets, we use the LHS method to generate 1,000 variables in each time slot. Figures 5(a), 5(b), and 5(c) represent the boxplots of the WP values at each hour with errors of 10%, 15%, and 20%, respectively. Fifty deterministic solutions (DS) in Case 1 and fifty robust solutions (RS) in Case 2 (WP error of 10%) shown in Figure 4 are used for the robustness analysis. As generator G1 is assumed to be a slack generator, its output is determined by other decision variables and WP output. The adaptive adjustment of the slack generator allows the dispatch solutions to adapt to other WP scenarios. Twenty new stochastic scenarios from the boxplots with a 10% WP error in Figure 5(a) are selected for the case study. Figure 6 shows the Boxplot for function values of DS and RS under worse case on twenty 24-hour WP stochastic scenarios. It is clearly that most f_1 and f_2 values of

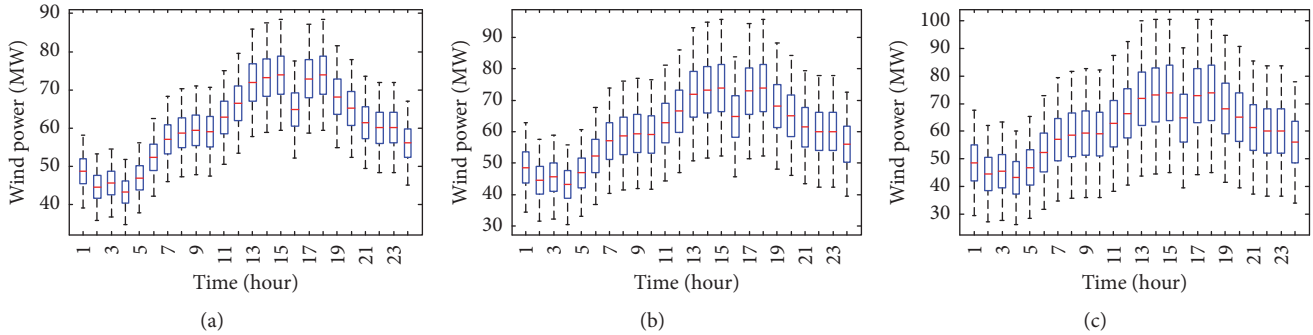

Figure 5: Boxplot for the wind power at each hour: WP error of (a) 10%; (b) 15%; and (c) 20%.

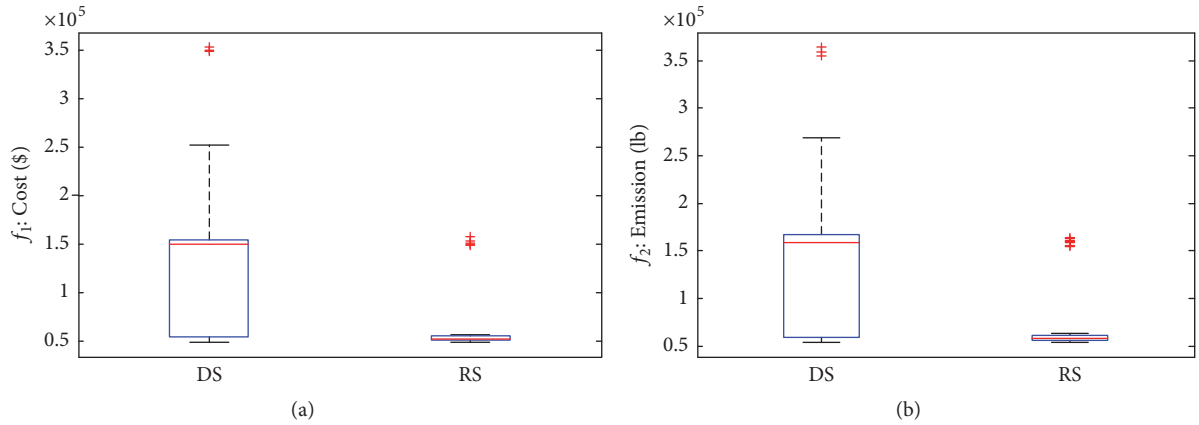

Figure 6: Boxplot for results of deterministic solutions (DS) and robust solutions (RS): (a) f_1 (cost); (b) f_2 (emission).

DS are larger than the penalty coefficient C (1E5). However, the f_1 and f_2 values of the Pareto front in Figure 4 with a 10% WP error are smaller than the penalty coefficient C (1E5). This means that most DS are not all feasible simultaneously for twenty 24-hour WP stochastic scenarios and punished by the penalty when dealing with the dispatch problem with a 10% WP error. Most of RS in Figure 6 are feasible and less sensitive to WP changes. It is proved that RS have a better robustness to uncertain WP.

6.3. Generators and ES Dispatch Analysis. The generators and ES dispatch of the compromise solutions [11] in Case 1 and in the scenario of Case 2 (10% WP error) are given as the examples in Tables 3 and 4, respectively. All generator outputs and ES at each time period properly satisfy the output limits. The functional values are smaller than the penalty coefficient C (1E5), which reveals that no constraints are violated. This means that the constraints have been properly handled.

The results of the ES dispatch analyses are reported in this part. The compromise solutions from the PSO-TLBO in Tables 3 and 4 are listed for the ES SOC analysis. Figure 7 reports the daily SOC profiles during the entire dispatch process. Under the SOC profiles with relevant ES dispatch patterns in Figure 7, ES helps to successfully ensure that all system operation constraints are satisfied during all intervals and to improve the economic and environmental benefits. As foreseeable in Figure 7, the SOC varies within the admissible range between 0.2 and 1. The ES works in charging mode followed by discharging mode and is then charged to the same SOC level as the initial SOC. The ES nearly follows this same pattern each day. The ES has an average of one complete charge-discharge cycle every day. Therefore, the ES constraints in each period, and over the entire dispatch period, are properly satisfied.

6.4. ES Benefits Analysis. ES in this paper is used for simultaneously improving flexibility of energy dispatch and peak shaving. To test the benefits of ES, the deterministic dispatch without WP error and the robust dispatch with a 15% WP error but without ES in Case 3 are shown in this part. The Pareto solutions of EED problem with ES and without ES are compared in Figures 8(a) and 8(b), respectively. It is observed that the Pareto solutions without ES are dominated by the Pareto solutions with ES. The results reveal the test without ES performance worse in minimizing f_1 and f_2 compared with that with ES in both cases. This is because the dispatch problem becomes more flexible and generators with lower cost and emission can be better utilized when ES is incorporated. Also, peak shaving characteristics of compromise dispatch solutions in Cases 1 and 2 are shown in Table 5 with respect to the distance ratio between peak to valley in (26). It is clear in Table 5 that the demands at the peak hours decrease and shift to the valley periods when ES is incorporated.

Table 3: Dispatch of the compromise solution in Case 1 ($f_1 = 5.08 \times 10^4$ \$, $f_2 = 5.81 \times 10^4$ lb).

Time (hour)	G1	G2	G3	G4	G5	G6	ES
1	53.27	30.85	41.48	28.48	26.9	24.44	−12.61
2	45.88	46.27	26.49	23.02	38.86	42.25	−9.72
3	38.99	45.65	32.56	39.6	45.32	42.52	−8.33
4	40.78	45.11	64.94	39	60.48	38.59	−9.57
5	88.32	66.12	72.25	53.66	63.38	69.15	−54.33
6	97.2	56.28	59.75	71.9	72.63	64.73	−4.86
7	106.61	86.18	83.87	105.92	64.47	73.74	−9.28
8	127.06	116.34	93.11	100.54	73.32	84.63	13.41
9	124.86	109.06	89.42	105.96	86.69	94.63	29.77
10	120.41	102.49	70.25	141.36	94.7	87.39	8.52
11	136.58	103.87	89.66	129.37	98.85	79.82	24.15
12	135.9	82.26	68.89	113.08	92.82	94.07	30.02
13	128.22	104.8	93.64	105.04	84.43	88.42	31.17
14	132.36	84.37	80.3	115.45	77.72	87.26	0.28
15	115.21	95.3	83.49	106.53	76.27	83.03	0.19
16	91.46	103.48	78.6	107.01	99	81.27	0.05
17	118.7	103.1	71.09	127.9	92.72	80.86	0
18	154.22	109.19	85.57	102.39	92.99	99.43	0
19	139.11	111.71	88.38	127.77	98.15	100.93	0
20	140.49	98.68	78.61	123.96	93.34	90.99	9.64
21	137.55	101.58	71.77	112.9	103.39	83.06	−3.45
22	122.81	68.01	89.6	93.44	96.03	57.54	−18.33
23	100.69	64.17	72.42	90.62	75.74	76.17	−28.42
24	93.36	79.35	51.95	83.01	51.45	61.56	−15.01

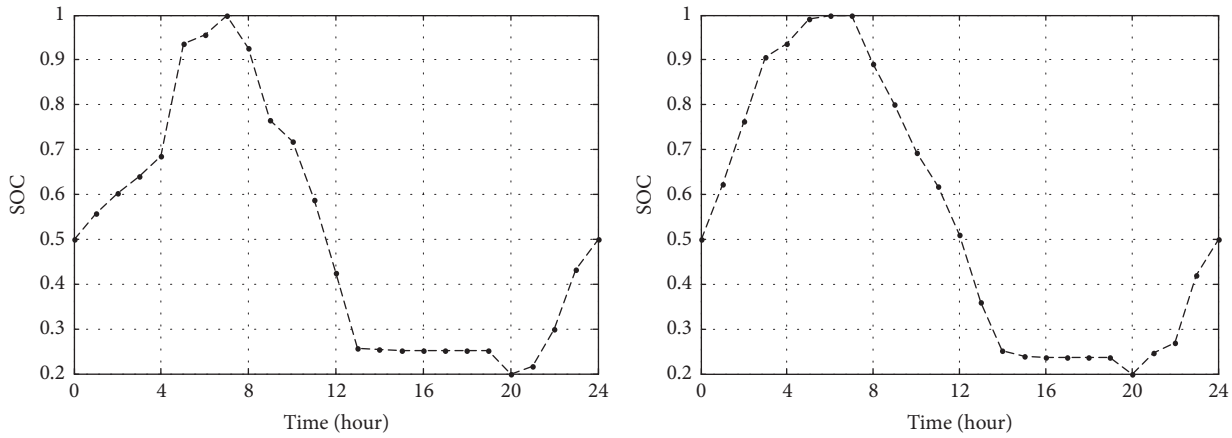

(a) Without WP error (b) With 10% WP error

Figure 7: ES SOC at different scenarios in Cases 1 and 2 with 10% WP error.

$$\text{peak to valley\%} = 100 \times \left(\frac{d^{\max}(t) - d^{\min}(t)}{d^{\max}(t)} \right). \quad (26)$$

6.5. Comparison of PSO-TLBO with TV-MOPSO. To investigate the performance of the PSO-TLBO algorithm in the multiobjective, day-ahead dispatch problem, comparison simulations for Cases 1 and 2 are studied. One of the most popular and effective multiobjective PSO algorithms, the TV-MOPSO [42], is used for the comparison. The typical Pareto fronts using two algorithms on the aforementioned cases are shown in Figure 9. We observe from the subfigures in Figure 9 that most of the solutions obtained with the TV-MOPSO are dominated by those achieved with the PSO-TLBO. It is observed that the TV-MOPSO performs worse when finding the whole Pareto front. The multiobjective PSO-TLBO has been found to have better convergence and better spread solutions compared with the TV-MOPSO in both cases. This

Table 4: Dispatch of compromise solution in Case 2 with 10% WP error ($f_1 = 5.40 \times 10^4$ \$, $f_2 = 5.89 \times 10^4$ lb).

Time (hour)	G1	G2	G3	G4	G5	G6	ES
1	67.44	31.08	28.13	39.32	36.69	26.67	−26.51
2	46.61	64.89	40.54	26.51	30.4	44.1	−30.9
3	38.48	55.98	36.54	52.33	51.71	41.29	−30.64
4	77.74	47.07	33.83	40.97	44.74	50.78	−6.84
5	72.70	70.97	50.29	71.59	62.51	50.34	−11.63
6	78.61	75.09	40.84	93.95	60.51	81.07	−2.17
7	81.01	72.53	75.83	122.63	92.47	78.24	0
8	112.36	85.84	100.78	123.58	94.26	83.11	20.16
9	119.64	115.73	90.14	131.42	90.07	89.42	16.44
10	125.53	107.33	91.92	122.56	84.18	84.98	20.01
11	137.45	117.5	103.57	131.07	84.56	87.13	14
12	112.97	111.29	103.12	119.69	75.22	87.97	19.73
13	121.49	111.47	96.76	120.98	85.95	85.91	27.72
14	109.81	93.87	93.1	94.69	94.94	85.2	19.76
15	113.29	78.4	85.93	122.17	88.09	84.79	2.41
16	118.15	102.18	75.63	108.19	79.71	90.43	0.11
17	107.40	119.08	107.5	97.57	92.2	84.85	0.04
18	137.97	119.81	114.21	121.28	79.75	85.1	0.02
19	150.10	114.49	81.82	134.86	91.27	107.44	0.27
20	123.53	103.15	88.78	140.77	95.99	89.9	6.54
21	104.54	112.51	95.79	118.86	98.05	98.86	−9.87
22	93.75	89.26	96.22	90.31	79.08	76.69	−5.15
23	61.87	74.43	94.08	103.8	90.16	71.67	−32.87
24	65.48	67.08	72.02	90.89	67.11	71.49	−17.33

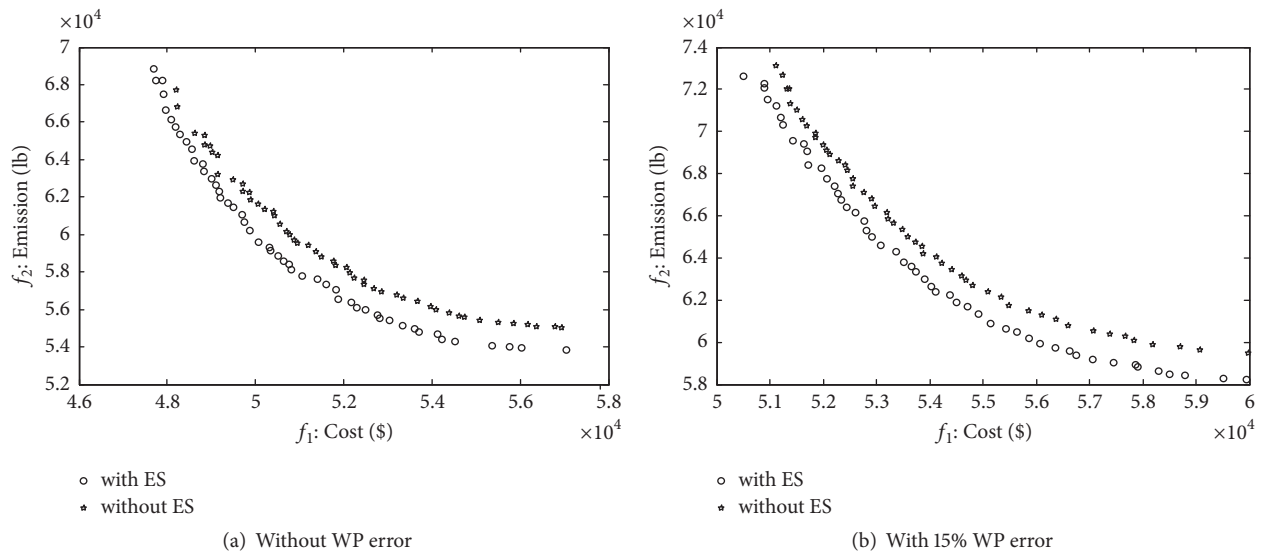

(a) Without WP error

(b) With 15% WP error

Figure 8: Pareto fronts obtained in scenarios with ES and without ES from the PSO-TLBO.

is because that hybrid PSO-TLBO search strategy and CCS strategy in multiobjective PSO-TLBO algorithm promote the population diversity. They are helpful in improving the search ability. The performance of multiobjective PSO-TLBO has been improved by comparing with single PSO evolution. Hence, the PSO-TLBO performs well in solving day-ahead EED dispatch problems.

7. Conclusion

The increasing development and penetration of REG are a major challenge for transmission and distribution networks. ES presents the potential to supportively optimize system operations with REG and reduce other excessive participations to grid operation, such as voltage and VAR

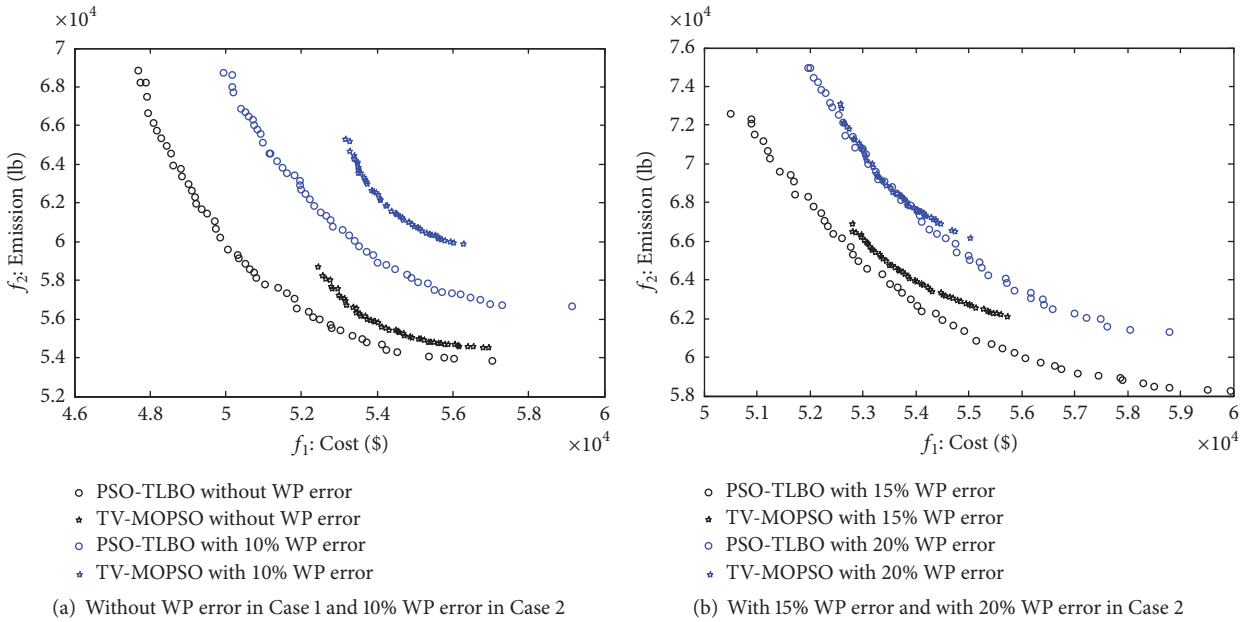

(a) Without WP error in Case 1 and 10% WP error in Case 2

(b) With 15% WP error and with 20% WP error in Case 2

Figure 9: Pareto fronts obtained using the PSO-TLBO and TV-MOPSO in Cases 1 and 2.

Table 5: Peak to valley in different scenarios.

Scenarios	Peak to valley%
Without ES	66.67%
Case 1 without WP error	64.92%
Case 2 with 10% WP error	62.97%
Case 2 with 15% WP error	63.81%
Case 2 with 20% WP error	62.96%

regulation. In this paper, based on conventional EED experiences, we combine a robust, multiobjective optimization method and an EED problem formulation to solve the day-ahead ES dispatch problem with REG uncertainty. The robust optimal dispatch solutions are adaptive to uncertain REG and only one generator (slack generator) production needs to be adjusted. The numerical study explores the different WP prediction errors on the impact of the robust objective function values. The results show that a higher WP prediction error will lead to more economic cost and greater emissions. Moreover, the ES dispatch patterns provide ancillary services, such as peak shaving, to provide economic, emission, and technical benefits. The simulation case results also reveal that the multiobjective PSO-TLBO performs well in solving robust EED dispatch problems compared with TV-MOPSO.

In future research, the complex dispatch tasks require more objective functions that could be added, such as the REG penetration rate, and carbon emission, especially technical objective functions. The proposed robust generators and ES dispatch method can be verified in real power system with a high penetration of REG, and REG curtailment can be considered. Moreover, the increasing number of ES deployments to active distribution networks will be an increasingly complex problem. These will be dealt with in the future improvements.

Conflicts of Interest

The authors declare that there are no conflicts of interest.

Acknowledgments

This work was supported by the National Natural Science Foundation of China under Grant no. 51177177, National "111" Project of China under Grant no. B08036, and the Science and Technology Project of State Grid Corporation of China under Grant no. 5220001600V6 (Key Technology of the Optimal Allocation and Control of Distributed Energy Storage Systems in Energy Internet).

References

[1] H. Zhang, D. Yue, and X. Xie, "Robust Optimization for Dynamic Economic Dispatch under Wind Power Uncertainty with Different Levels of Uncertainty Budget," *IEEE Access*, vol. 4, pp. 7633–7644, 2016.

[2] X. Li, J. Lai, and R. Tang, "A Hybrid Constraints HANdling Strategy for MULticonstrained MULtiobjective Optimization Problem of MICrogrid Economical/ENVironmental Dispatch," *Complexity*, Art. ID 6249432, 12 pages, 2017.

[3] T. Niknam and H. Doagou-Mojarrad, "Multiobjective economic/emission dispatch by multiobjective θ-particle swarm optimisation," *IET Generation, Transmission & Distribution*, vol. 6, no. 5, pp. 363–377, 2012.

[4] N. A. Khan, G. A. S. Sidhu, and F. Gao, "Optimizing Combined Emission Economic Dispatch for Solar Integrated Power Systems," *IEEE Access*, vol. 4, pp. 3340–3348, 2016.

[5] M. Zheng, X. Wang, C. J. Meinrenken, and Y. Ding, "Economic and environmental benefits of coordinating dispatch among distributed electricity storage," *Applied Energy*, vol. 210, pp. 842–855, 2018.

[6] J. S. Dhillon, S. C. Parti, and D. P. Kothari, "Stochastic economic emission load dispatch," *Electric Power Systems Research*, vol. 26, no. 3, pp. 179–186, 1993.

[7] J. Y. Fan and L. Zhang, "Real-time economic dispatch with line flow and emission constraints using quadratic programming," *IEEE Transactions on Power Systems*, vol. 13, no. 2, pp. 320–325, 1998.

[8] J. X. Xu, C. S. Chang, and X. W. Wang, "Constrained multiobjective global optimisation of longitudinal interconnected power system by genetic algorithm," *IEE Proceedings—Generation, Transmission & Distribution*, vol. 143, no. 5, pp. 435–446, 1996.

[9] T. D. King, M. E. El-Hawary, and F. El-Hawary, "Optimal environmental dispatching of electric power systems via an improved hopfield neural network model," *IEEE Transactions on Power Systems*, vol. 10, no. 3, pp. 1559–1565, 1995.

[10] P. S. Kulkarni, A. G. Kothari, D. P. K, "Combined Economic and Emission Dispatch Using Improved Backpropagation Neural Network," *Electric Machines & Power Systems*, vol. 28, no. 1, pp. 31–44, 2010.

[11] L. H. Wu, Y. N. Wang, X. F. Yuan, and S. W. Zhou, "Environmental/economic power dispatch problem using multiobjective differential evolution algorithm," *Electric Power Systems Research*, vol. 80, no. 9, pp. 1171–1181, 2010.

[12] Z. Lu, S. He, T. Feng, X. Li, X. Guo, and X. Sun, "Robust economic/emission dispatch considering wind power uncertainties and flexible operation of carbon capture and storage," *International Journal of Electrical Power & Energy Systems*, vol. 63, pp. 285–292, 2014.

[13] M. S. Li, Q. H. Wu, T. Y. Ji, and H. Rao, "Stochastic multiobjective optimization for economic-emission dispatch with uncertain wind power and distributed loads," *Electric Power Systems Research*, vol. 116, pp. 367–373, 2014.

[14] H. Zhao, Q. Wu, S. Hu, H. Xu, and C. N. Rasmussen, "Review of energy storage system for wind power integration support," *Applied Energy*, vol. 137, pp. 545–553, 2015.

[15] X. Luo, J. Wang, M. Dooner, and J. Clarke, "Overview of current development in electrical energy storage technologies and the application potential in power system operation," *Applied Energy*, vol. 137, pp. 511–536, 2015.

[16] K. W. Wee, S. S. Choi, and D. M. Vilathgamuwa, "Design of a least-cost battery-supercapacitor energy storage system for realizing dispatchable wind power," *IEEE Transactions on Sustainable Energy*, vol. 4, no. 3, pp. 786–796, 2013.

[17] A. A. Moghaddam, A. Seifi, and T. Niknam, "Multi-operation management of a typical micro-grids using Particle Swarm Optimization: A comparative study," *Renewable & Sustainable Energy Reviews*, vol. 16, no. 2, pp. 1268–1281, 2012.

[18] K. Liu, K. Li, and C. Zhang, "Constrained generalized predictive control of battery charging process based on a coupled thermoelectric model," *Journal of Power Sources*, vol. 347, pp. 145–158, 2017.

[19] K. Liu, K. Li, Z. Yang, C. Zhang, and J. Deng, "An advanced Lithium-ion battery optimal charging strategy based on a coupled thermoelectric model," *Electrochimica Acta*, vol. 225, pp. 330–344, 2017.

[20] Y. Xu and Z. Li, "Distributed Optimal Resource Management Based on the Consensus Algorithm in a Microgrid," *IEEE Transactions on Industrial Electronics*, vol. 62, no. 4, pp. 2584–2592, 2015.

[21] H. Ma, Z. Yang, P. You, and M. Fei, "Multi-objective biogeography-based optimization for dynamic economic emission load dispatch considering plug-in electric vehicles charging," *Energy*, vol. 135, pp. 101–111, 2017.

[22] M. Mahmoodi, P. Shamsi, and B. Fahimi, "Economic dispatch of a hybrid microgrid with distributed energy storage," *IEEE Transactions on Smart Grid*, vol. 6, no. 6, pp. 2607–2614, 2015.

[23] H. Chen, R. Zhang, G. Li, L. Bai, and F. Li, "Economic dispatch of wind integrated power systems with energy storage considering composite operating costs," *IET Generation, Transmission & Distribution*, vol. 10, no. 5, pp. 1294–1303, 2016.

[24] R. Rigo-Mariani, B. Sareni, X. Roboam, and C. Turpin, "Optimal power dispatching strategies in smart-microgrids with storage," *Renewable & Sustainable Energy Reviews*, vol. 40, pp. 649–658, 2014.

[25] N. Yan, Z. X. Xing, W. Li, and B. Zhang, "Economic Dispatch Application of Power System with Energy Storage Systems," *IEEE Transactions on Applied Superconductivity*, vol. 26, no. 7, 2016.

[26] Q. Wang, J. Wang, and Y. Guan, "Stochastic unit commitment with uncertain demand response," *IEEE Transactions on Power Systems*, vol. 28, no. 1, pp. 562-563, 2013.

[27] M. H. Alham, M. Elshahed, D. K. Ibrahim, and E. E. D. Abo El Zahab, "A dynamic economic emission dispatch considering wind power uncertainty incorporating energy storage system and demand side management," *Journal of Renewable Energy*, vol. 96, pp. 800–811, 2016.

[28] J. Hetzer, D. C. Yu, and K. Bhattarai, "An economic dispatch model incorporating wind power," *IEEE Transactions on Energy Conversion*, vol. 23, no. 2, pp. 603–611, 2008.

[29] C. Chen, S. Duan, T. Cai, B. Liu, and G. Hu, "Optimal allocation and economic analysis of energy storage system in microgrids," *IEEE Transactions on Power Electronics*, vol. 26, no. 10, article no. 43, pp. 2762–2773, 2011.

[30] G. Carpinelli, G. Celli, S. Mocci, F. Mottola, F. Pilo, and D. Proto, "Optimal integration of distributed energy storage devices in smart grids," *IEEE Transactions on Smart Grid*, vol. 4, no. 2, pp. 985–995, 2013.

[31] A. Gabash and P. Li, "Flexible optimal operation of battery storage systems for energy supply networks," *IEEE Transactions on Power Systems*, vol. 28, no. 3, pp. 2788–2797, 2013.

[32] A. Gabash and P. Li, "Active-reactive optimal power flow in distribution networks with embedded generation and battery storage," *IEEE Transactions on Power Systems*, vol. 27, no. 4, pp. 2026–2035, 2012.

[33] Z. Li, W. Wu, B. Zhang, and B. Wang, "Adjustable Robust Real-Time Power Dispatch with Large-Scale Wind Power Integration," *IEEE Transactions on Sustainable Energy*, vol. 6, no. 2, pp. 357–368, 2015.

[34] R. MA, K. LI, X. LI, and Z. QIN, "An economic and low-carbon day-ahead Pareto-optimal scheduling for wind farm integrated power systems with demand response," *Journal of Modern Power Systems and Clean Energy*, vol. 3, no. 3, pp. 393–401, 2015.

[35] Y. S. Ong, P. B. Nair, and K. Y. Lum, "Max-min surrogate-assisted evolutionary algorithm for robust design," *IEEE Transactions on Evolutionary Computation*, vol. 10, no. 4, pp. 392–404, 2006.

[36] S. Salomon, G. Avigad, P. J. Fleming, and R. C. Purshouse, "Active robust optimization: Enhancing robustness to uncertain environments," *IEEE Transactions on Cybernetics*, vol. 44, no. 11, pp. 2221–2231, 2014.

[37] K. Mason, J. Duggan, and E. Howley, "Multi-objective dynamic economic emission dispatch using particle swarm optimisation variants," *Neurocomputing*, vol. 270, pp. 188–197, 2017.

[38] Z. Yang, K. Li, Q. Niu, and Y. Xue, "A comprehensive study of economic unit commitment of power systems integrating various renewable generations and plug-in electric vehicles," *Energy Conversion and Management*, vol. 132, pp. 460–481, 2017.

[39] J. J. Liang, A. K. Qin, P. N. Suganthan, and S. Baskar, "Comprehensive learning particle swarm optimizer for global optimization of multimodal functions," *IEEE Transactions on Evolutionary Computation*, vol. 10, no. 3, pp. 281–295, 2006.

[40] F. Zou, L. Wang, X. Hei, D. Chen, and B. Wang, "Multi-objective optimization using teaching-learning-based optimization algorithm," *Engineering Applications of Artificial Intelligence*, vol. 26, no. 4, pp. 1291–1300, 2013.

[41] T. Cheng, M. Chen, P. J. Fleming, Z. Yang, and S. Gan, "A novel hybrid teaching learning based multi-objective particle swarm optimization," *Neurocomputing*, vol. 222, pp. 11–25, 2017.

[42] P. K. Tripathi, S. Bandyopadhyay, and S. K. Pal, "Multi-objective particle swarm optimization with time variant inertia and acceleration coefficients," *Information Sciences*, vol. 177, no. 22, pp. 5033–5049, 2007.